Highly Efficient Dehydrogenation of Primary Aliphatic Alcohols Catalyzed by Cu Nanoparticles Dispersed on Rod-Shaped La$_2$O$_2$CO$_3$

Fei Wang,[†] Ruijuan Shi,[†] Zhi-Quan Liu,*[‡] Pan-Ju Shang,[‡] Xueyong Pang,[‡] Shuai Shen,[†] Zhaochi Feng,[†] Can Li,*[†] and Wenjie Shen*[†]

[†]State Key Laboratory of Catalysis, Dalian Institute of Chemical Physics, Chinese Academy of Sciences, Dalian 116023, China
[‡]Shenyang National Laboratory for Materials Science, Institute of Metal Research, Chinese Academy of Sciences, Shenyang 110016, China

Ⓢ *Supporting Information*

ABSTRACT: Copper nanoparticles dispersed rod-shaped La$_2$O$_2$CO$_3$ efficiently catalyzed transfer dehydrogenation of primary aliphatic alcohols with an aldehyde yield of up to 97%. This high efficiency was achieved by creating a catalytically active nanoenvironment for effective reaction coupling between alcohol dehydrogenation and styrene hydrogenation via hydrogen transfer. The {110} planes on the La$_2$O$_2$CO$_3$ nanorods not only provided substantial amounts of medium-strength basic sites for the activation of alcohol but also directed the selective dispersion of hemispherical Cu particles of about 4.5 nm on their surfaces, which abstracted and transferred hydrogen atoms for styrene hydrogenation. This finding provides a new strategy for developing highly active alcohol-dehydrogenation catalysts by tuning the shape of the oxide support and consequently the metal-oxide interfacial nanostructure.

KEYWORDS: heterogeneous catalysis, dehydrogenation, primary aliphatic alcohol, reaction coupling, Cu/La$_2$O$_2$CO$_3$ catalyst, crystal-facet selective deposition, active nanoenvironmental
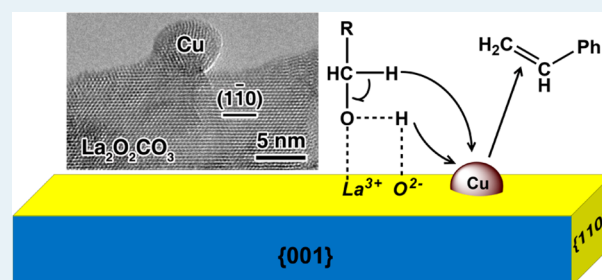
Dehydrogenation of primary aliphatic alcohols to aldehydes is of great importance in synthetic chemistry and fine chemical industry. This conversion is traditionally accomplished by oxidizing alcohols with stoichiometric amounts of chromate or permanganate,[1] generating large amounts of highly toxic heavy metal wastes. Oxidative dehydrogenation of alcohols using solid catalysts and atmospheric air or molecular oxygen avoids the environmental problem, producing water as the only byproduct in principle.[2] Supported Au,[3] Pd,[4] Pt,[5] and Ru[2b] catalysts are basically active for oxidative dehydrogenation of benzylic and allylic alcohols, known as activated alcohols, but are less active for primary aliphatic alcohols that are generally viewed as nonactivated alcohols. The practical application of oxidative dehydrogenation of alcohols is still hindered by the unsatisfied selectivity toward carbonyls and the safety concern linked with the use of flammable solvents under oxidative atmospheres.

Transfer dehydrogenation of alcohols that uses recyclable solid catalysts and unsaturated organic compounds as the hydrogen acceptors improves the selectivity of carbonyls and overcomes the safety problem, providing a new route for alcohol transformation. However, only a few heterogeneous catalysts are known to be effective for this novel conversion of alcohols, mostly activated alcohols. Pd nanoparticles catalyzed transfer dehydrogenation of allylic and aromatic alcohols using ethylene, cyclohexene, and nitrobenzene as the hydrogen acceptors.[6] Cu catalysts showed high activities in transfer dehydrogenation of secondary aliphatic alcohols using styrene as the hydrogen acceptor.[7] Hydrotalcite-supported Ag,[8] Au,[9] and Cu[10] particles and water-soluble Ru nanoparticles[11] effectively catalyzed oxidant-free dehydrogenations of secondary aliphatic and benzylic alcohols. Recently, copper particles supported on basic metal oxides were found to show remarkably enhanced activities in alcohol dehydrogenation.[12] Even though, efficient dehydrogenation of primary aliphatic alcohols is still challenging. In a previous study, we reported that a Cu/La$_2$O$_3$ catalyst offered a 1-octanal yield of 63% in transfer dehydrogenation of 1-octanol.[12c] Here, we further demonstrate that precisely tuning the chemical phase and the shape of the oxide support could significantly promote the efficiency of the Cu particles of 4−5 nm for transfer dehydrogenation of primary aliphatic alcohols, attaining an aldehyde yield of 97% under the optimized reaction conditions.

We started with the synthesis of La(OH)$_3$ nanorods using a hydrothermal process. The nanorods had widths of 10−15 nm and lengths of 200−400 nm (Supporting Information, Figure S1). Calcination of this lanthanum hydroxide precursor at 773 K for 4 h in air yielded La$_2$O$_2$CO$_3$ nanorods with straight sides and regular ends (Supporting Information, Figure S2). Figure 1a is a high-resolution transmission electron microscopy

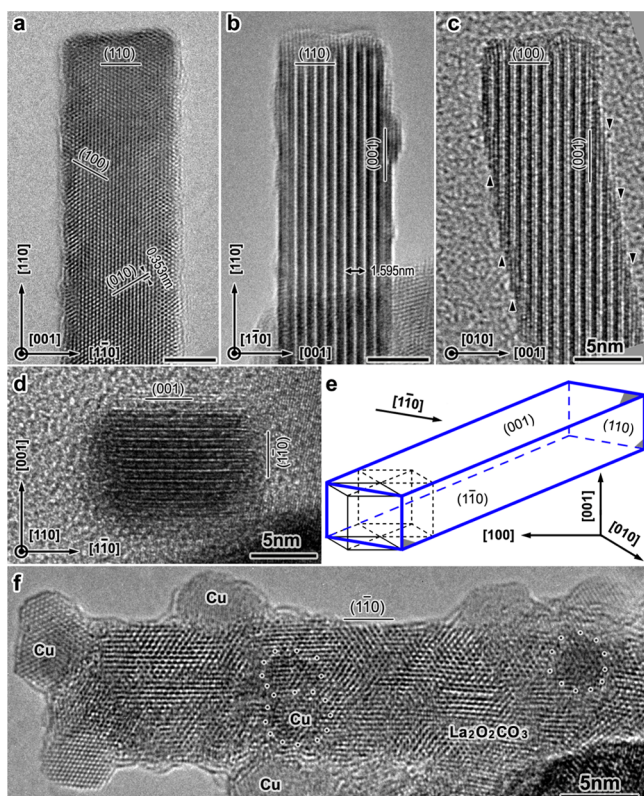**Figure 1.** HRTEM images of the $La_2O_2CO_3$ nanorod viewed along the (a) [001], (b) [1$\bar{1}$0], and (c) [010] orientations. The arrow-heads in panel c indicate the steps on the (001) plane, noticing that at these steps La and O atoms in the (110) plane are exposed to the surface. (d) A rectangular cross-section (10 × 15 nm) of the nanorod viewed near the [110] orientation. (e) Illustration of the real shape of the $La_2O_2CO_3$ nanorod. (f) Hemispherical Cu particles with a mean size of about 4.5 nm on the $La_2O_2CO_3$ nanorod viewed along the [001] orientation; the dotted circles referred to the copper nanoparticles on the (001) flat plane.

(HRTEM) image of a single $La_2O_2CO_3$ nanorod viewed along the [001] orientation. The nanorod grew along the [110] direction and was enclosed by (110), (100), and (010) planes. HRTEM images viewed along the [1$\bar{1}$0] (Figure 1b) and [010] (Figure 1c) orientations verified the dominant exposure of (001) planes. When viewed along the growing direction of [110] (Figure 1d), the nanorod had a rectangular cross-section with (1$\bar{1}$0) and (001) side planes. Taking all these observations into account, the real shape of the $La_2O_2CO_3$ nanorod was assumed to be a square block that was terminated by two (001) flat planes, two (1$\bar{1}$0) side planes, and two (110) end planes, as illustrated in Figure 1e where the hexagonal unit was outlined. The width of the flat (001) plane was about 15 nm while that of the side (1$\bar{1}$0) plane was about 10 nm. Hemispherical Cu nanoparticles with an average size of 4.5 nm were then dispersed on the $La_2O_2CO_3$ nanorods by a deposition-precipitation method. Figure 1f shows a HRTEM image of the $Cu/La_2O_2CO_3$ catalyst. There were only a few Cu particles deposited on the (001) flat planes as indicated with dotted circles; most Cu nanoparticles were preferentially anchored on the {110} surfaces, including the (1$\bar{1}$0) side planes and the (110) end planes (Supporting Information, Figure S3), showing a distinct crystal-facet selective deposition pattern. Since the {110} facet have a high energy,[13] preferential deposition of Cu particles minimized the overall surface energy.

Meanwhile, the favorable lattice matching between the Cu (111) and the $La_2O_2CO_3$ (110) may also result in a selective deposition of copper particles.

The $Cu/La_2O_2CO_3$ catalyst showed exceptionally high activity in transfer dehydrogenation of 1-octanol, the most frequently used representative of primary aliphatic alcohols. In a preliminary test, 1-octanol was dehydrogenated to 1-octanal with a yield of 8% at 373 K; the yield of 1-octanal increased when raising the temperature and reached 64% at 413 K (Supporting Information, Table S1). Optimization of the styrene/1-octanol molar ratio and the reaction time resulted in 1-octanal yield of 97% at 423 K (Table 1). By adding styrene as

Table 1. Transfer Dehydrogenation of 1-Octanol on the Cu/$La_2O_2CO_3$ Catalyst at 423 K[a]

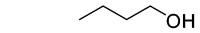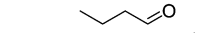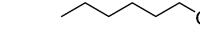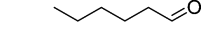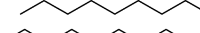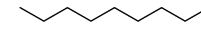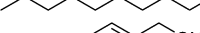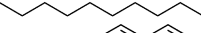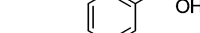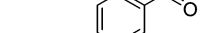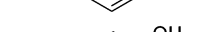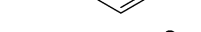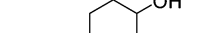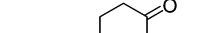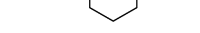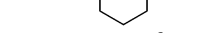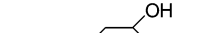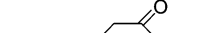| entry	time (h)	S/O (ratio)[b]	conv. (%)	select. (%)	yield (%)
1	3	1.0	72	100	72
2	3	2.0	84	>99	83
3	3	4.0	87	99	86
4	8	4.0	94	99	93
5	10	4.0	98	99	97

[a]Reaction conditions: $Cu/La_2O_2CO_3$ (200 mg), 1-octanol (2 mmol), mesitylene (8 mL), styrene (2–8 mmol), N_2 atmosphere. [b]Styrene/1-octanol molar ratio.

the hydrogen acceptor in an equimolar ratio with respect to 1-octanol, the yield of 1-octanal was 72% and increased to 83% by using 2 equivalent moles of styrene. Further increasing the styrene/1-octanol molar ratio to 4.0 only slightly promoted 1-octanal yield to 86%. When prolonging the reaction time, the yield of 1-octanal increased moderately from 86% at 3 h to 97% at 10 h. In these experiments, the number of moles of ethylbenzene produced approximately equaled to that of 1-octanol converted. This result evidenced the effective reaction coupling between 1-octanol dehydrogenation and styrene hydrogenation through hydrogen transfer.

The $Cu/La_2O_2CO_3$ catalyst was also highly active for transfer dehydrogenation of other primary aliphatic alcohols (Table 2). Dehydrogenations of 1-butanol and 1-hexanol produced the corresponding aldehydes with the yields of 84% and 93%, respectively. For the dehydrogenation of higher C-chain alcohols, like 1-decanol and 1-dodecanol, the aldehyde yields approached 74–85%. These slightly lowered yields might be due to the relatively slow surface migration of the bulky substrates on the catalyst surface.[14] The scope of the substrate could be extended to primary aromatic and cycloaliphatic alcohols. Transfer dehydrogenation of benzyl alcohol, the typical substrate of primary aromatic alcohols, provided benzylaldehyde yields of 58% at 383 K for 6 h and 100% at 423 K for 1 h. Moreover, primary cycloaliphatic alcohols, like cyclohexanol and cyclooctanol, were easily dehydrogenated to cycloaliphatic aldehydes with yields of 61–99% at 383 K. Most interestingly, the $Cu/La_2O_2CO_3$ catalyst was also effective for transfer dehydrogenation of primary benzylic alcohols. 2-Phenyl-ethanol, whose dehydrogenation is more challenging than that of primary aliphatic alcohols, was converted to 2-acetonaphthone with the yields of 11% at 383 K for 7 h and 52% at 423 K for 6 h. As expected, secondary aliphatic alcohols (2-octanol) and activated aromatic alcohols (1-phenyl-2-

Table 2. Transfer Dehydrogenation of Alcohols on the Cu/La$_2$O$_2$CO$_3$ Catalyst[a]

Entry	Substrate	Product	T (K)	Time (h)	Conv. (%)	Select. (%)	Yield (%)
1	(primary alcohol)	(aldehyde)	423	8	85	>99	84
2	(primary alcohol)	(aldehyde)	423	8	93	100	93
3	(primary alcohol)	(aldehyde)	423	8	85	100	85
4	(primary alcohol)	(aldehyde)	423	8	75	100	75
5	benzyl alcohol	benzaldehyde	383	6	58	100	58
			423	1	100	100	100
6	cyclohexanol	cyclohexanone	383	5	61	100	61
			423	8	91	>99	90
7	cyclooctanol	cyclooctanone	383	1	100	>99	99
8	2-phenylethanol	phenylacetaldehyde	383	7	11	100	11
			423	6	52	100	52
9	2-octanol	2-octanone	383	1	100	100	100
10	1-phenylethanol	acetophenone	383	1	100	100	100

[a]Reaction conditions: Cu/La$_2$O$_2$CO$_3$ (200 mg), alcohol (2 mmol), styrene (8 mmol), mesitylene (8 mL), N$_2$ atmosphere.

ethanol) were fully dehydrogenated to the corresponding carbonyls at 383 K within 1 h on the Cu/La$_2$O$_2$CO$_3$ catalyst.

The outstanding performance of the Cu/La$_2$O$_2$CO$_3$ catalyst in transfer dehydrogenation of primary aliphatic alcohols is understandable on the basis of the reaction mechanisms derived from classical studies carried out for homogeneous and heterogeneous dehydrogenations of alcohols. In homogeneous catalysis, to achieve satisfactorily high alcohol conversion and/ or aldehyde selectivity, organic bases or alkaline compounds were often added to the reaction media for expediting the deprotonation of the alcoholic group.[15] When heterogeneous catalysts are used, alcohol was activated by interacting with the surface oxygen on the supporting oxides, acting as a Brønsted base. The high activities of gold, silver, and copper nanoparticles in oxidant-free dehydrogenation of alcohols were primarily assigned to the basic sites on the hydrotalcites.[8c] Our previous study on a Cu/La$_2$O$_3$ catalyst for transfer dehydrogenation of 1-octanol verified the importance of the basic sites on the La$_2$O$_3$ surface covered by La$_2$O$_2$CO$_3$ species and the maximum yield of 1-octanal approached 63% under the optimal conditions.[12c] Here, tuning the shape of the supporting La$_2$O$_2$CO$_3$ further promoted the 1-octanal yield to a level of 97% under the optimized conditions, presumably due to the variations in the basic properties associated with the dominant exposure of the {110} facets. Temperature-programmed desorption of CO$_2$ on the Cu/La$_2$O$_2$CO$_3$ catalyst showed an intense desorption peak at about 560 K (Figure 2a), indicating the presence of substantial amounts of medium-strength basic sites (La^{3+}-O^{2-} pairs).[16] Crystallographically, La$_2$O$_2$CO$_3$ has a hexagonal structure where each La^{3+} cation is surrounded by seven oxygen anions: four in tetrahedral and three in octahedral coordinations. As mentioned above, the La$_2$O$_2$CO$_3$ nanorod was enclosed by two end (110) planes, two (1$\bar{1}$0) side planes, and two (001) flat planes. Our density-functional theory calculations identified that the {110} planes were made up of O and La atoms whereas the {001} plane contained O and C

atoms only (Figure 2b and Supporting Information, Figure S4). Since the surface area of the {110} planes was about 40% of the total surface area, the coordinatively unsaturated O^{2-} sites or La^{3+}-O^{2-} pairs on the {110} facets predominantly contributed to the overall basicity of the La$_2$O$_2$CO$_3$ nanorods.

Infrared spectroscopy of 1-octanol adsorption on the catalyst evidenced that the La$_2$O$_2$CO$_3$ nanorod activated alcohol while the Cu nanoparticle facilitated hydrogen transfer (Figure 2c and Supporting Information, Figure S5). On bare La$_2$O$_2$CO$_3$ nanorods, 1-octanol was dissociatively activated through the interaction of its O−H bond with the surface La^{3+}-O^{2-} pairs at 423 K, forming alkoxide species (La−O−CH$_2$−R at 1046 cm^{-1}).[17a] On the Cu/La$_2$O$_2$CO$_3$ catalyst, however, the stretching modes of the −CH$_2$ groups have blue-shifted by 5 cm^{-1}; the La−O−CH$_2$−R band on bare La$_2$O$_2$CO$_3$ vanished, but a new band at 1078 cm^{-1} representing Cu−O−CH$_2$−R-like species[17b] appeared, indicating that the copper particle abstracted another hydrogen atom from the α-C−H bond and activated the C−O bond in the adsorbed alkoxide intermediate. These results suggest that transfer dehydrogenation of 1-octanol on the Cu/La$_2$O$_2$CO$_3$ catalyst follows a bifunctional mechanism involving both the Cu nanoparticle and the La$_2$O$_2$CO$_3$ nanorod (Figure 2d). The first hydrogen atom was removed from the alcoholic group by the basic sites on the La$_2$O$_2$CO$_3$ nanorod, forming alkoxide species. The abstraction of the α-hydrogen from the alkoxide was then accomplished on the nearby copper particle, producing aldehyde. Simultaneously, the Cu particle catalyzed styrene hydrogenation using the hydrogen atoms released from the alcohol, driving the reaction equilibrium toward aldehyde. In such a reaction model, the {110} plane on the La$_2$O$_2$CO$_3$ nanorod not only provided sufficient basic sites for the primary activation of the alcohol but also directed the preferential dispersion of Cu particles on its surface, creating a synergetic nanoenvironment for the efficient reaction coupling between 1-octanol dehydrogenation and styrene hydrogenation through hydrogen transfer.
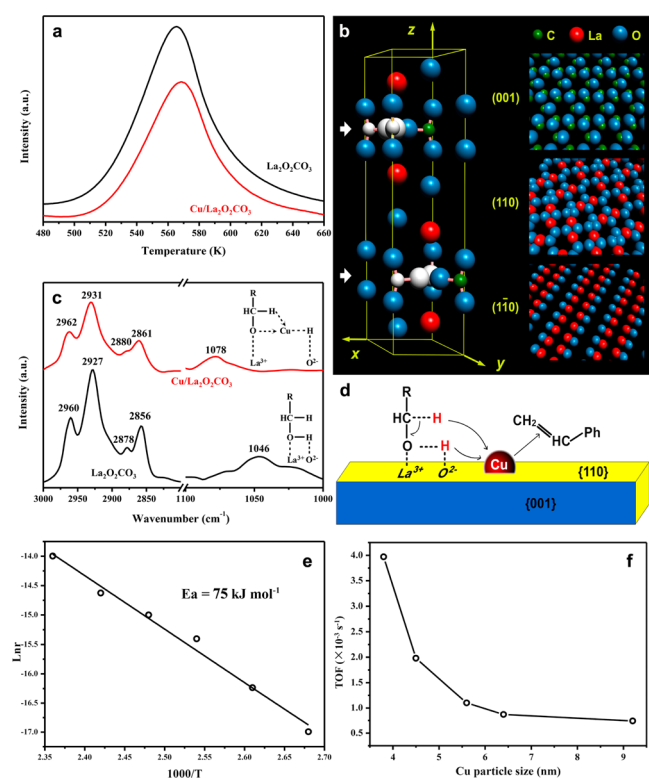
Figure 2. Possible reaction pathway of 1-octanol transfer dehydrogenation. (a) Profiles of temperature-programmed desorptions of CO_2 on the $La_2O_2CO_3$ nanorods (black curve) and the $Cu/La_2O_2CO_3$ catalyst (red curve); the intense desorption peaks at about 560 K represented the medium-strength basic sites (La^{3+}-O^{2-} pairs) with a total amount of 0.16 mmol·g^{-1} on the $La_2O_2CO_3$ nanorods and 0.11 mmol·g^{-1} on the $Cu/La_2O_2CO_3$ catalyst. (b) Hexagonal unit of $La_2O_2CO_3$ crystal (left) in which the C and O atomic sites are 1/3 occupied at the arrow-indicated sublayers (the gray ball refers as to the vacancies), and the atomic arrangements (right) of the {001} and {110} planes. (c) IR spectra of 1-octanol adsorption on bare $La_2O_2CO_3$ nanorods (black curve) and the $Cu/La_2O_2CO_3$ (red curve) at 423 K. (d) A depicting scheme of 1-octanol dehydrogenation on the Cu nanoparticle and the {110} plane of the $La_2O_2CO_3$. (e) Arrhenius plot of the reaction rate on the $Cu/La_2O_2CO_3$ catalyst at 373−423 K. (f) TOFs as a function of copper particle size at 423 K.

Kinetic measurements identified that the activation energy for the transfer dehydrogenation of 1-octanol was 75 kJ mol^{-1} on the $Cu/La_2O_2CO_3$ catalyst in the temperature range of 373−423 K, which is very similar to that of the previous Cu/La_2O_3 catalyst (Supporting Information, Figure S6). However, the reaction rate on the $Cu/La_2O_2CO_3$ catalyst was much higher than that on the Cu/La_2O_3 catalyst; it increased from 4.17×10^{-8} mol g^{-1} s^{-1} at 373 K to 8.33×10^{-7} mol g^{-1} s^{-1} at 423 K (Figure 2e and Supporting Information, Table S2), probably because of the high density of basic sites on the $La_2O_2CO_3$ nanorods (Supporting Information, Figure S6). The reaction rate also strongly depended on the size of the Cu particles involved in hydrogen transfer and styrene hydrogenation. When increasing the size from 3.8 to 5.6 nm, the turnover frequency (TOF) decreased dramatically from 3.97×10^{-3} s^{-1} to 1.10×10^{-3} s^{-1} at 423 K, but further increasing the size of copper particle to 9.2 nm only moderately lowered the TOF to 7.41×10^{-4} s^{-1} (Figure 2f and Supporting Information, Table S3). Control experiments confirmed the heterogeneous nature of the reaction (Supporting Information, Table S4).

Recycling tests verified that the current catalyst maintained high activity for five consecutive runs without decrease in the selectivity of 1-octanal (more than 99%). The slight decrease in 1-octanol conversion was assigned to the minor aggregation of copper nanoparticles (Supporting Information, Figure S7).

On the basis of these findings, we conclude that Cu nanoparticles selectively dispersed on the {110} facets of $La_2O_2CO_3$ nanorods are highly active for transfer dehydrogenation of primary aliphatic alcohols. The medium-strength basic sites on the {110} facets of the rod-shaped $La_2O_2CO_3$ interacted strongly with Cu nanoparticles, generating a catalytically active nanoenvironment for the reaction coupling between alcohol dehydrogenation and styrene hydrogenation. This strategy raises the prospect of using nanostructured solid catalysts for the efficient dehydrogenation of alcohols to functionalized carbonyls, and consequently contributes to the sustainable development of green chemistry.

■ ASSOCIATED CONTENT

ⓢ Supporting Information

Materials and methods; additional experimental results in the structural analyses of the catalysts, dehydrogenations of different types of alcohols, reaction kinetics, and recycle tests. This material is available free of charge via the Internet at http://pubs.acs.org.

■ AUTHOR INFORMATION

Corresponding Author

*E-mail: shen98@dicp.ac.cn (W.S.), zqliu@imr.ac.cn (Z.-Q.L.), canli@dicp.ac.cn (C.L.).

Notes

The authors declare no competing financial interest.

■ ACKNOWLEDGMENTS

■ REFERENCES

(1) Hudlicky, M. *Oxidations in organic chemistry*; American Chemical Society: Washington, DC, 1990.

(2) (a) Mallat, T.; Baiker, A. *Chem. Rev.* **2004**, *104*, 3037. (b) Matsumoto, T.; Uneo, M.; Wang, N.; Kobayashi, S. *Chem.—Asian J.* **2008**, *3*, 196. (c) Prabhakaran, V. C.; Lee, W. K.; Adam, F. J. *Chem. Technol. Biotechnol.* **2011**, *86*, 161.

(3) (a) Abad, A.; Concepcion, P.; Corma, A.; Garcia, H. *Angew. Chem., Int. Ed.* **2005**, *44*, 4066. (b) Su, F. Z.; Liu, Y. M.; Wang, L. C.; Cao, Y.; He, H. Y.; Fan, K. N. *Angew Chem., Int. Ed.* **2008**, *47*, 334. (c) Boronat, M.; Corma, A.; Illas, F.; Radilla, J.; Ródenas, T.; Sabater, M. J. *J. Catal.* **2011**, *278*, 50. (d) Costa, V. V.; Estrada, M.; Demidova, Y.; Prosvirin, I.; Kriventsov, V.; Costa, R. F.; Fuentes, S.; Simakov, A.; Gusevskaya, E. V. *J. Catal.* **2012**, *292*, 148.

(4) (a) Mori, K.; Hara, T.; Mizugaki, T.; Ebitani, K.; Kaneda, K. *J. Am. Chem. Soc.* **2004**, *126*, 10657. (b) Meenakshisundaram, S.; Ewa, N.; Ramchandra, T. *Chem.—Eur. J.* **2011**, *17*, 6524.

(5) Yamada, Y. M. A.; Arakawa, T.; Hocke, H.; Uozumi, Y. *Angew Chem., Int. Ed.* **2007**, *46*, 704.

(6) (a) Hayashi, M.; Yamada, K.; Nakayama, S.; Hayashi, H.; Yamazaki, S. *Green Chem.* **2000**, *2*, 257. (b) Keresszegi, C.; Mallat, T.; Baiker, A. *New J. Chem.* **2001**, *25*, 1163. (c) Tanaka, T.; Kawabata, H.; Hayashi, M. *Tetrahedron Lett.* **2005**, *46*, 4989.

(7) (a) Zaccheria, F.; Ravasio, N.; Psaro, R.; Fusi, A. *Chem. Commun.* **2005**, 253. (b) Zaccheria, F.; Ravasio, N.; Psaro, R.; Fusi, A. *Chem.—Eur. J.* **2006**, *12*, 6426.

(8) (a) Mitsudome, T.; Mikami, Y.; Funai, H.; Mizugaki, T.; Jitsukawa, K.; Kaneda, K. *Angew. Chem., Int. Ed.* **2008**, *47*, 138. (b) Shimizu, K.; Sugino, K.; Sawabe, K.; Satsuma, A. *Chem.—Eur. J.* **2009**, *15*, 2341. (c) Kaneda, K.; Mitsudome, T.; Mizugaki, T.; Jitsukawa, K. *Molecules* **2010**, *15*, 8988.

(9) (a) Fang, W.; Zhang, Q.; Chen, J.; Deng, W.; Wang, Y. *Chem. Commun.* **2010**, 1547. (b) Fang, W.; Chen, J.; Zhang, Q.; Deng, W.; Wang, Y. *Chem.—Eur. J.* **2011**, *17*, 1247.

(10) Mitsudome, T.; Mikami, Y.; Ebata, K.; Mizugaki, T.; Jitsukawa, K.; Kaneda, K. *Chem. Commun.* **2008**, 4804.

(11) Feng, B.; Chen, C.; Yang, H.; Zhao, X.; Li, H.; Yu, Y.; Cao, T.; Shi, Y.; Hou, Z. *Adv. Synth. Catal.* **2012**, *354*, 1559.

(12) (a) Shi, R.; Wang, F.; Mu, X.; Li, Y.; Huang, X.; Shen, W. *Catal. Commun.* **2009**, *11*, 306. (b) Marella, R. K.; Neeli, C. K. P.; Kamaraju, S. R. R.; Burri, D. R. *Catal. Sci. Technol.* **2012**, *2*, 1833. (c) Shi, R.; Wang, F.; Ta, N.; Li, Y.; Huang, X.; Shen, W. *Green Chem.* **2010**, *12*, 108.

(13) Manoilova, O. V.; Podkolzin, S. G.; Tope, B.; Lercher, J.; Stangland, E. E.; Goupil, J. M.; Weckhuysen, B. M. *J. Phys. Chem. B* **2004**, *108*, 15770.

(14) Creyghton, E. J.; Downing, R. S. *J. Mol. Catal. A* **1998**, *134*, 47−61.

(15) Zhan, B. Z.; Thompson, A. *Tetrahedron* **2004**, *60*, 2917.

(16) (a) Shen, S. C.; Chen, X.; Kawi, S. *Langmuir* **2004**, *20*, 9130. (b) Olafsen, A.; Larsson, A. K.; Fjellvåg, H.; Hauback, B. C. *J. Solid State Chem.* **2001**, *158*, 14−24. (c) Hattori, H. *Chem. Rev.* **1995**, *95*, 537.

(17) (a) Wu, W. C.; Chuang, C. C.; Lin, J. L. *J. Phys. Chem. B* **2000**, *104*, 8719. (b) Fridman, V. Z.; Davydov, A. A.; Titievsky, K. *J. Catal.* **2004**, *222*, 545.